

Experiments and Computations for Inertial Confinement Fusion-Related Shock-Driven Hydrodynamic Instabilities

Bradley Motl, Devesh Ranjan, John Niederhaus, Jason Oakley, Mark Anderson, and Riccardo Bonazza

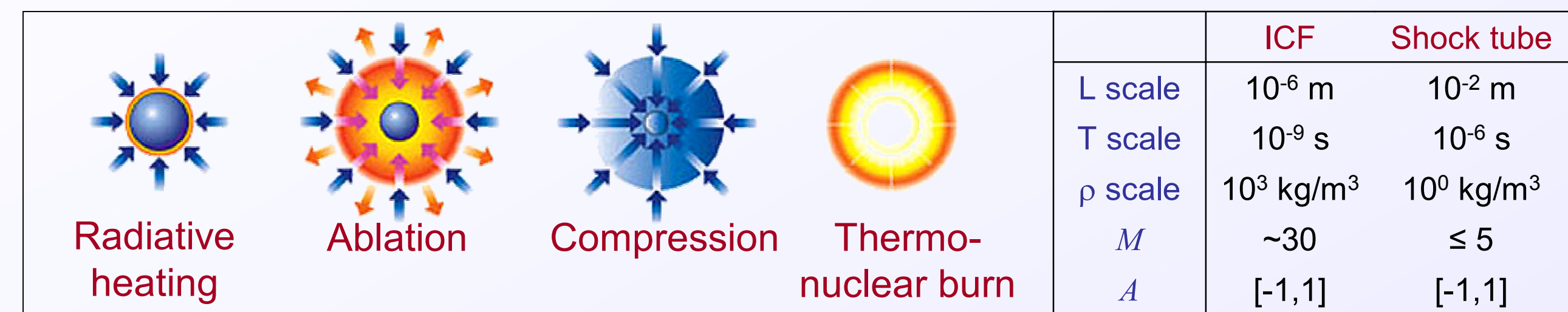
Fusion Technology Institute, University of Wisconsin-Madison

17th ANS Topical Meeting on the Technology of Fusion Energy, Albuquerque, NM, November 13-15, 2006



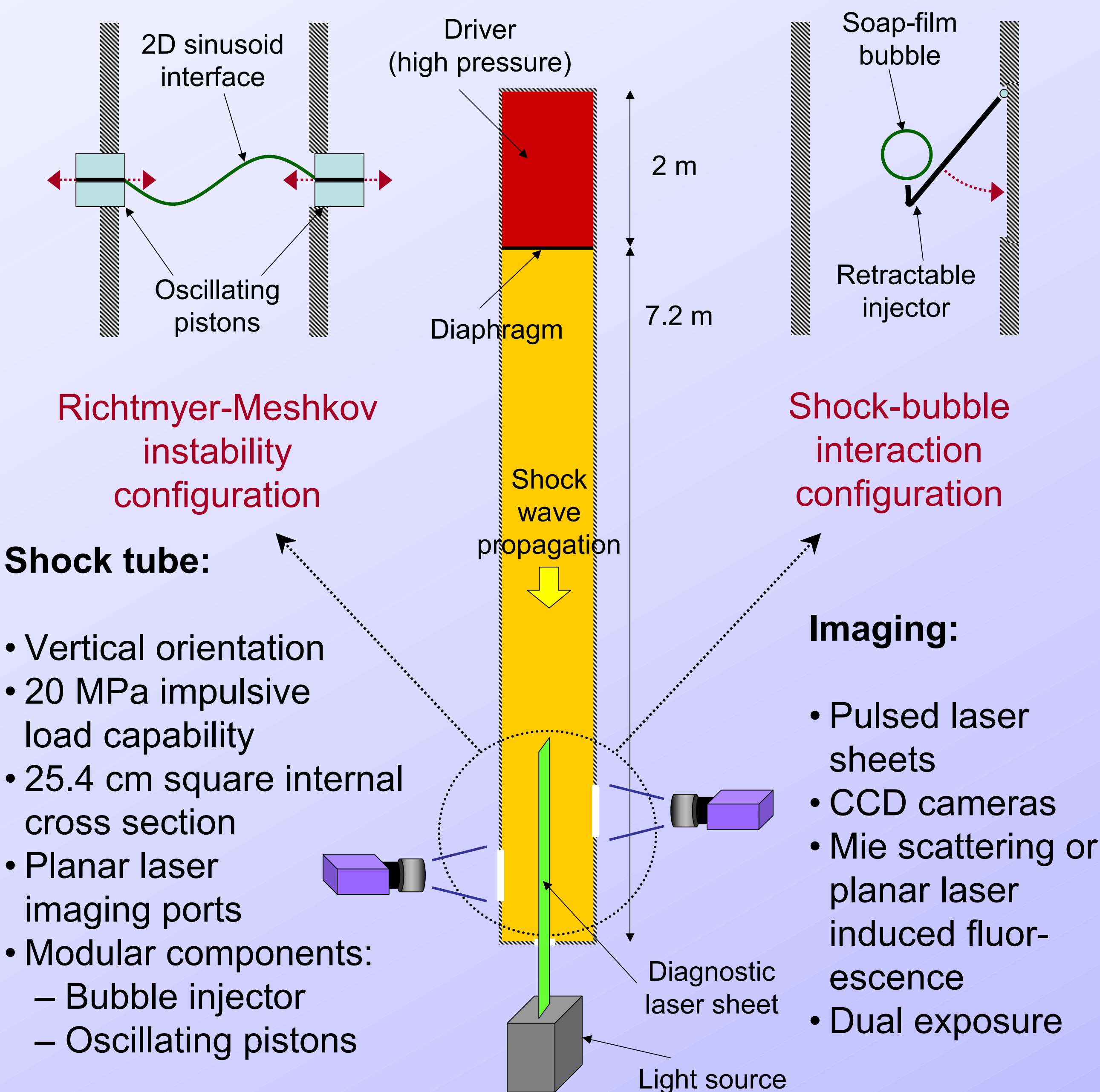
Relevance to ICF

In the inertial confinement (ICF) environment, shock-driven hydrodynamic instabilities and the associated mixing impose a limit on the efficiency with which fuel material may be compressed to the densities required for fusion, reducing the obtainable fusion yield. These instabilities arise at nonuniformities on density and material interfaces, as ablative and radiatively-driven shocks pass through the material and compress it, as shown below schematically.



In the present work, the phenomenology, mechanisms, and spatial and temporal scales of shock-driven instabilities are investigated using experiments in a gas shock tube environment, along with numerical simulations. In the shock tube environment, hydrodynamic phenomena may be characterized much more precisely than at ICF conditions, due to differences in conditions listed in the table above. Further, the absence of electric and magnetic fields, phase changes, and radiation allows purely hydrodynamic effects to be studied independently. Here, geometric length scales of the deformed interfaces are measured as indications of shock-induced mixing.

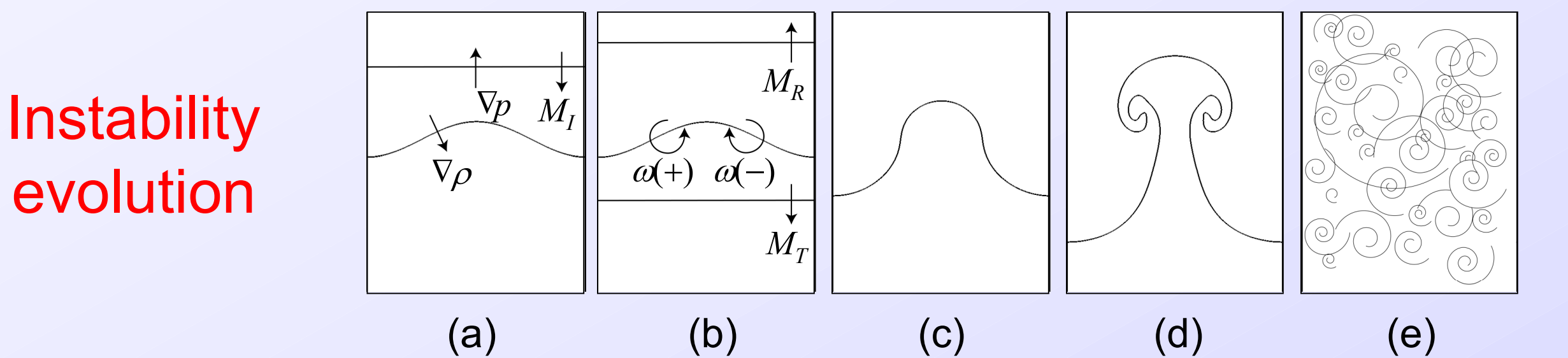
Wisconsin Shock Tube Laboratory



Introduction

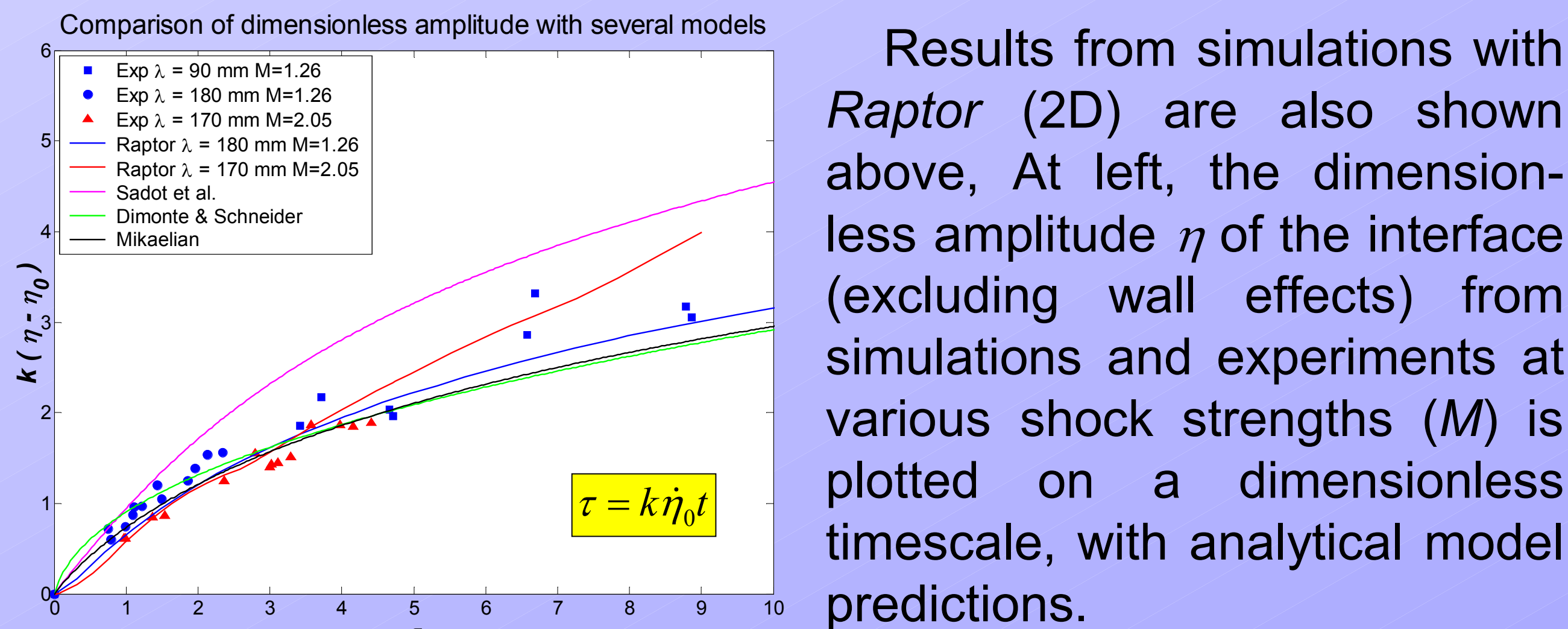
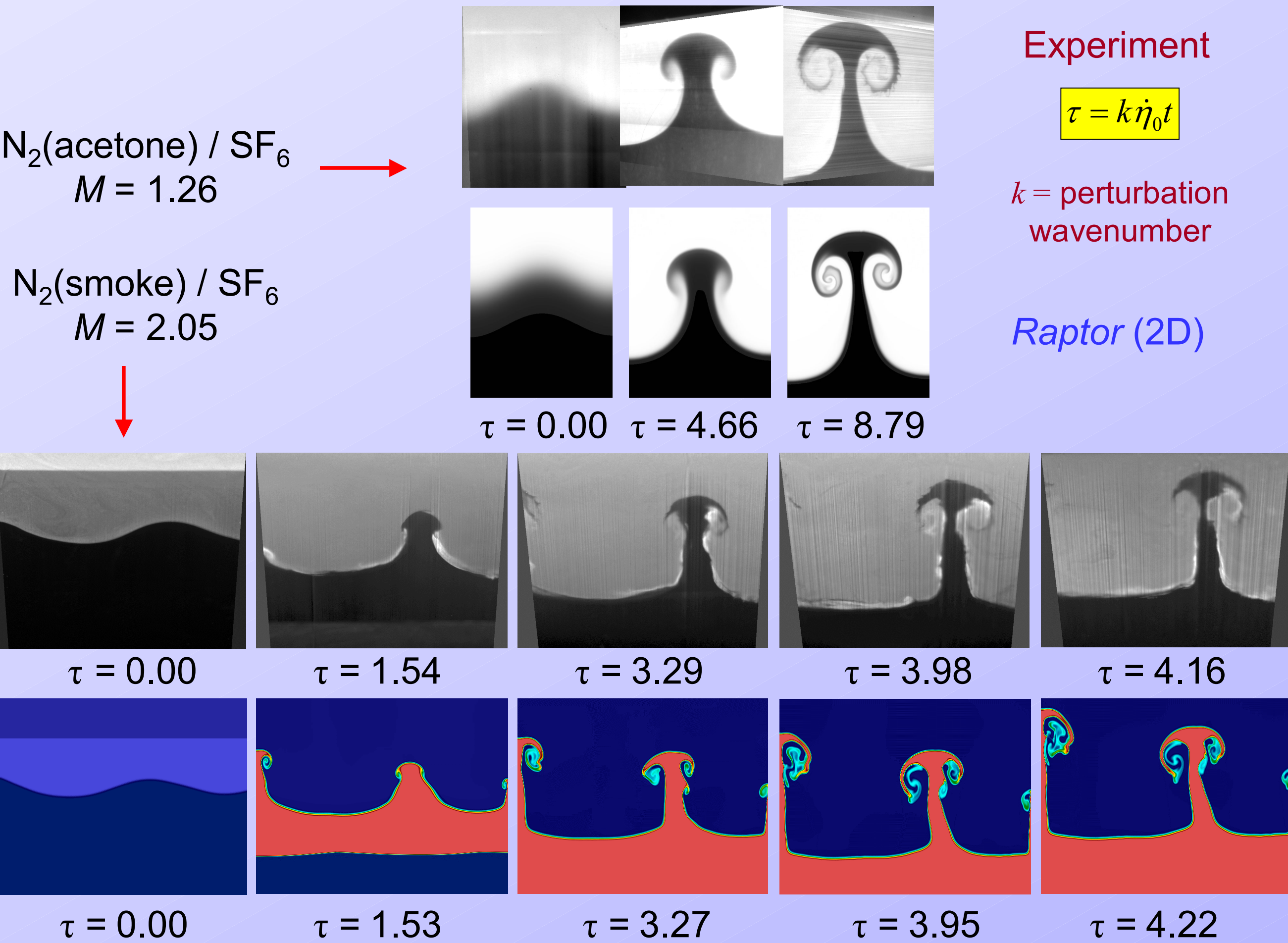
Shock-driven hydrodynamic instabilities are present in multi-component flows subjected to acceleration by shock waves. Vorticity is deposited on material interfaces baroclinically ($\nabla \rho \times \nabla p \neq 0$), causing interfaces to become unstable and deform. The geometric features of the deformed interfaces and mixing zones in two particular shock-driven flows are studied here: the Richtmyer-Meshkov instability of a planar interface with a small-amplitude sinusoidal perturbation, and the interaction of a planar shock wave with a discrete spherical bubble.

Richtmyer-Meshkov instability

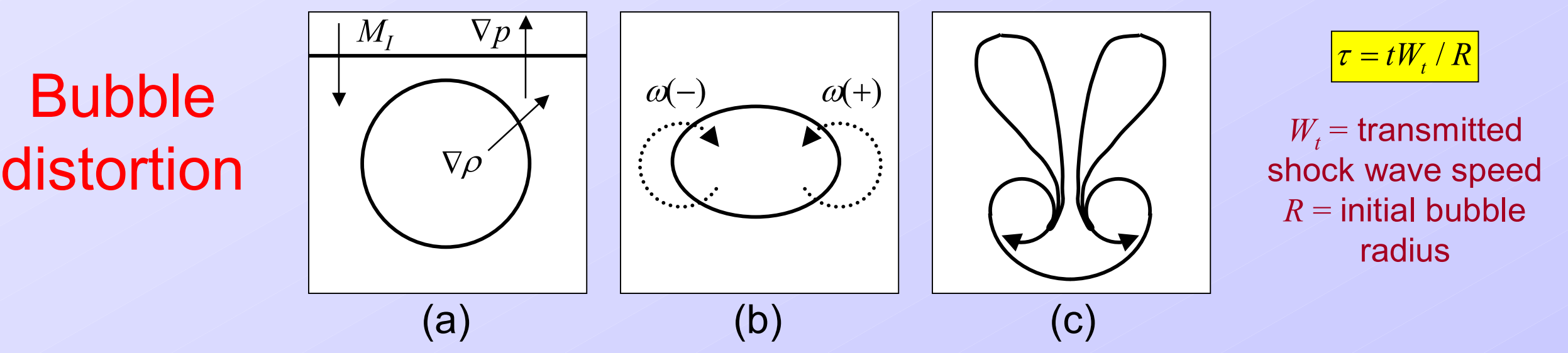


The evolution of the Richtmyer-Meshkov instability is shown schematically above: (a) initial configuration just prior to shock, (b) linear growth regime, (c) start of nonlinear growth, (d) appearance of mushroom structures, and (e) turbulent mixing.

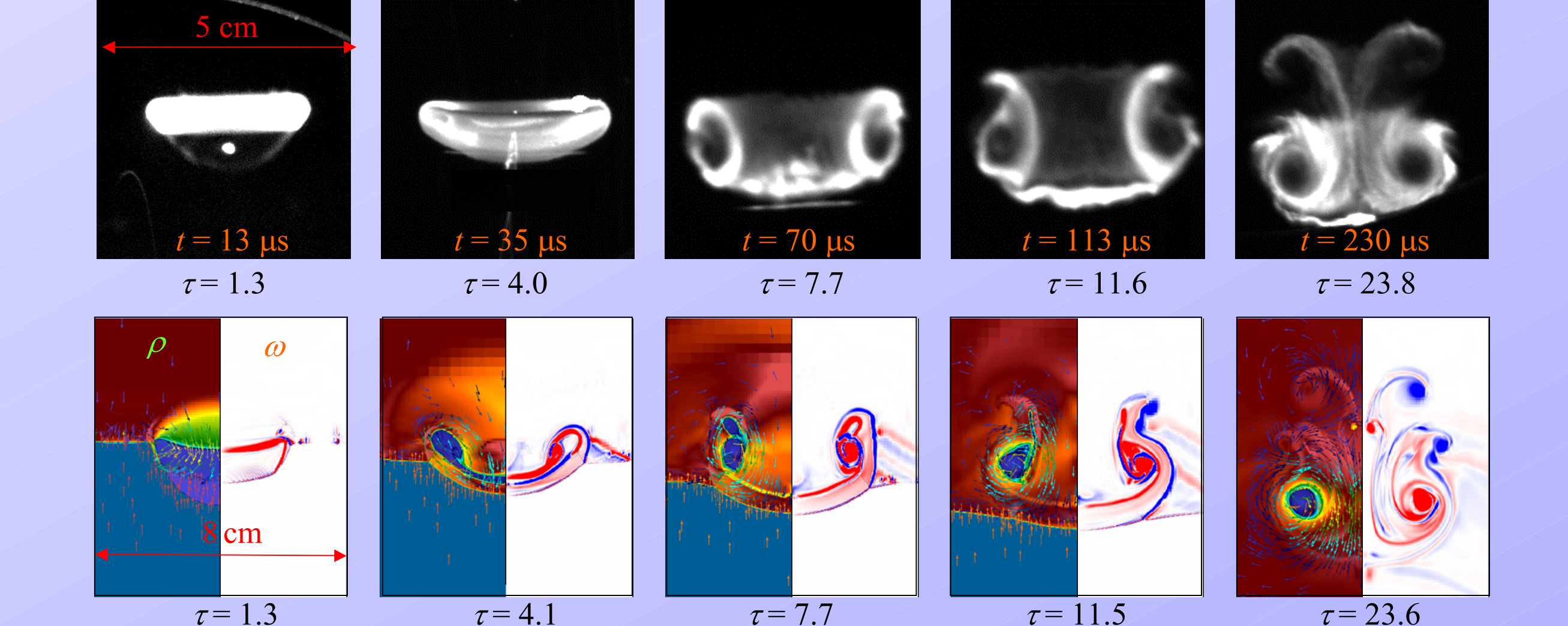
Below are images generated using planar laser diagnostics (PLIF or Mie scattering) from shock tube experiments studying the Richtmyer-Meshkov instability for a 2D sinusoidal interface between nitrogen (with flow tracer) above and SF₆ below.



Shock-bubble interaction

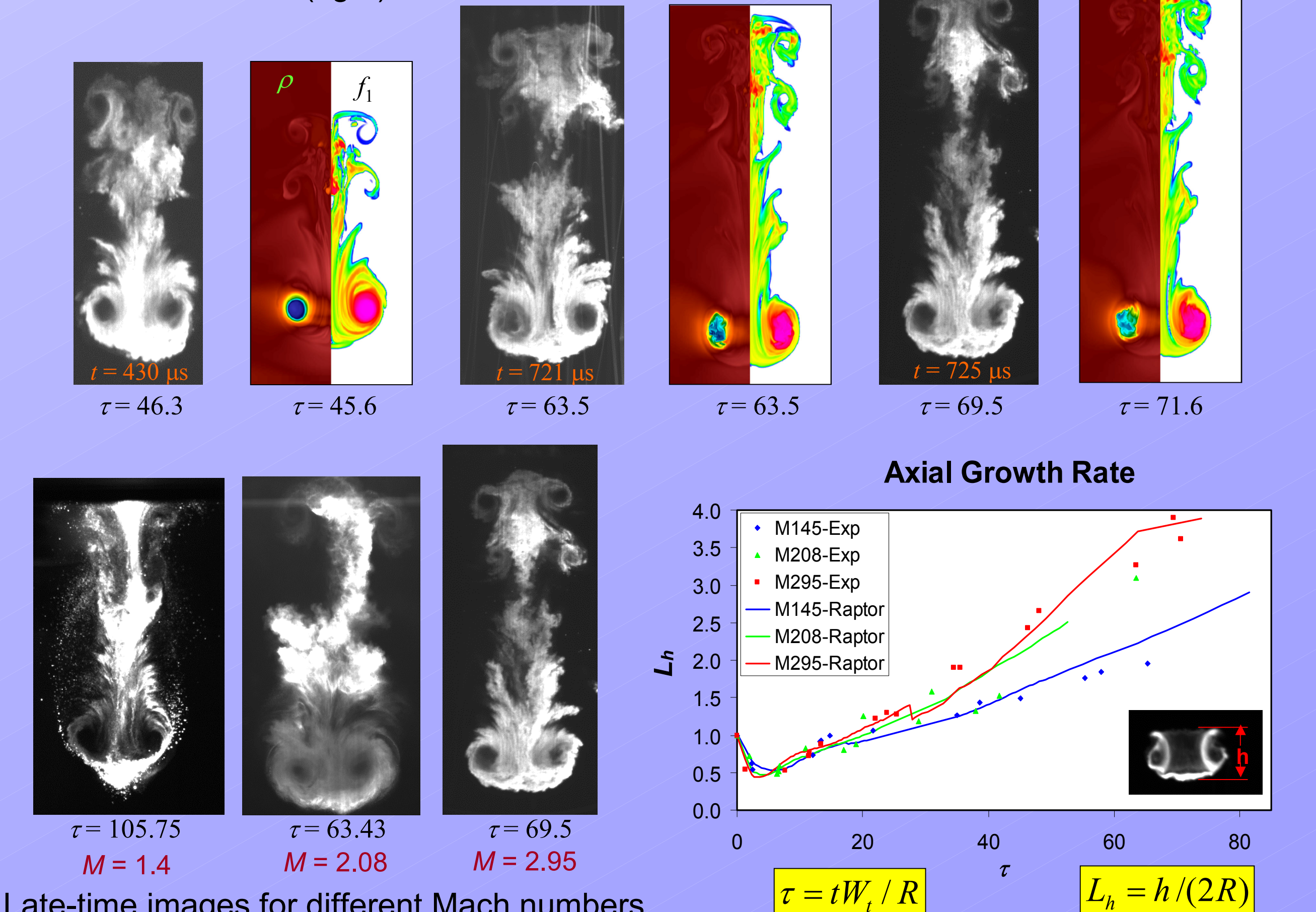


The evolution of a light bubble of initial radius R due to the interaction with a planar shock wave is shown schematically above: (a) initial configuration, (b) compression and rotation induced by shock passage, and (c) deformation and vortex ring formation.



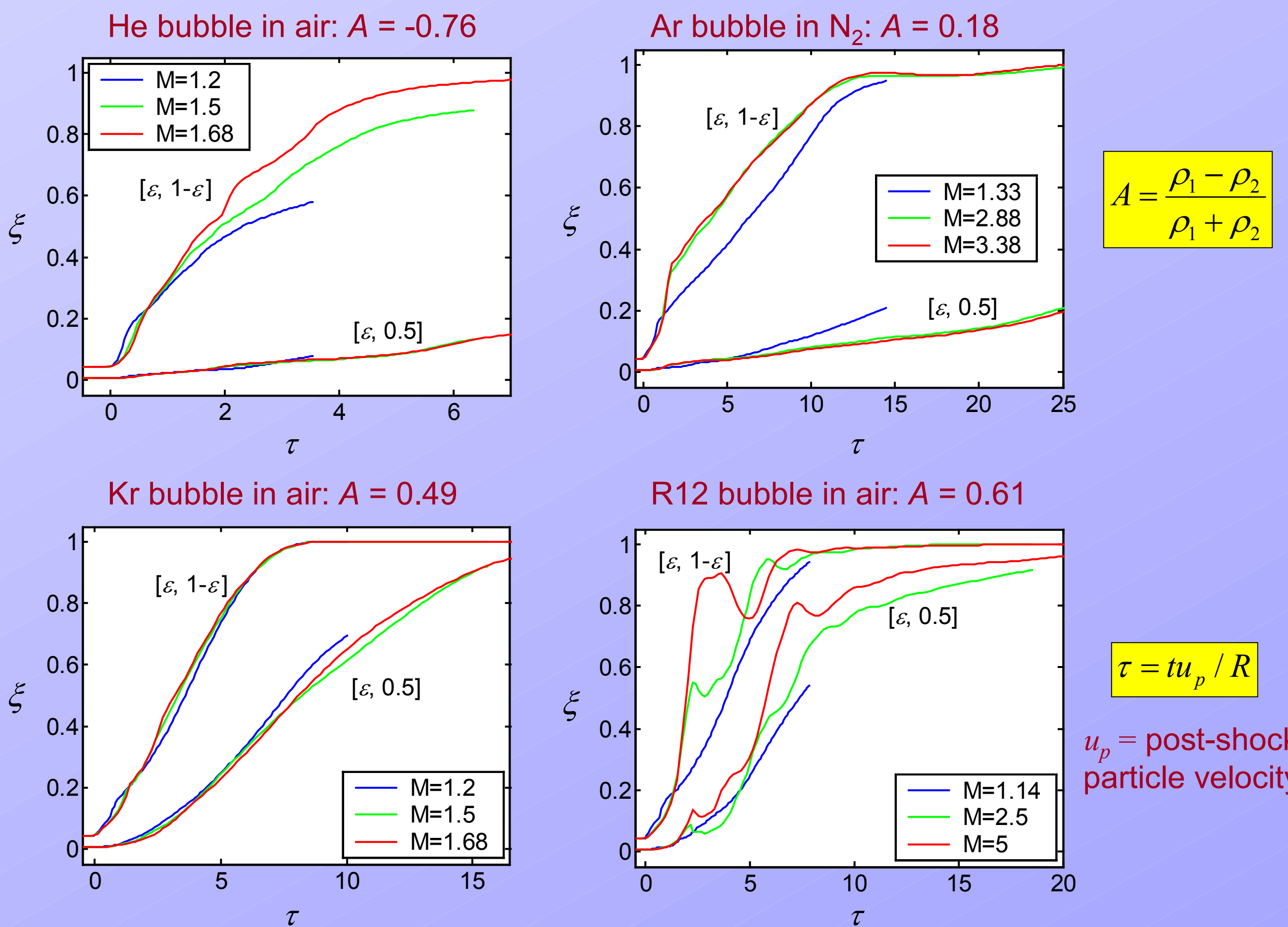
Top: experimental shock tube images obtained using laser light scattered at the bubble midplane for a helium bubble shocked at $M = 2.95$ in nitrogen. Bottom: results from 3D *Raptor* simulations: density (left) and vorticity magnitude (right) at bubble midplane.

Below: late-time experimental and numerical images showing multiple vortex rings and complex structure: total density (left) and bubble fluid volume fraction (right).



Computational parameter study

These flows are simulated numerically by integrating the 3D Euler equations using a piecewise-linear 2nd-order Godunov method with adaptive mesh refinement (AMR). The code is called *Raptor*, and was developed at LLNL and LBL (see Greenough, *et al.*). A computational parameter study was performed for the shock-bubble interaction, with 12 scenarios at $1.14 \leq M \leq 5$ and $-0.76 \leq A \leq 0.61$.



The results above show the growth of the mixed region within the shocked bubble as a function of dimensionless time, with M and A as parameters. This is quantified as ξ , where ξ is the ratio of the volume of mixed bubble gas to the total volume of bubble gas. The mixed volume is measured using concentration limits of $[\varepsilon, 1-\varepsilon]$ and $[\varepsilon, 0.5]$, where $\varepsilon = 1 \times 10^{-7}$. These data show that the intensity and extent of mixing increases with increasing values of the Atwood number A .

References

D. Ranjan, J. Niederhaus, B. Motl, M. Anderson, J. Oakley, and R. Bonazza, *Experimental investigation of primary and secondary features in high Mach number shock-bubble interaction*, Phys. Rev. Lett., in review (2006).

D. Ranjan, M. Anderson, J. Oakley, and R. Bonazza, *Experimental investigation of a strongly shocked gas bubble*, Phys. Rev. Lett., 94 (2005).

J. Niederhaus, D. Ranjan, J. Oakley, M. Anderson, and R. Bonazza, *Inertial-Fusion-Related Hydrodynamic Instabilities in a Spherical Gas Bubble Accelerated by a Planar Shock Wave*, Fusion Science and Technology 47, 4 (2005), p. 1160.

J. Greenough, J. Bell, and P. Colella, *An adaptive multi-fluid interface capturing method for compressible flows in complex geometry*, AIAA Paper 95-1718.

Acknowledgements

The authors would like to express sincere thanks to Jeff Greenough (LLNL), for facilitating computations, and Paul Brooks (UW-Madison) for developing and maintaining the experimental setup. This work was supported by US DOE Grant #DE-FG52-03NA00061.